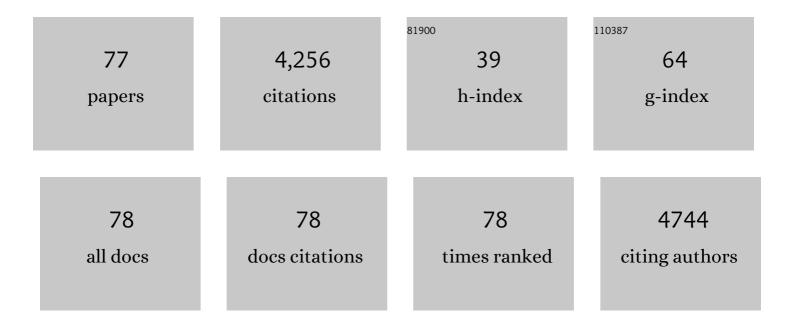
Aihua Liu

List of Publications by Year in descending order

Source: https://exaly.com/author-pdf/9221128/publications.pdf Version: 2024-02-01



#	Article	IF	CITATIONS
1	Accelerating the peroxidase-like activity of Co2+ by quinaldic acid: Mechanism and its analytical applications. Talanta, 2022, 239, 123080.	5.5	2
2	Hierarchical porous MoS2 particles: excellent multi-enzyme-like activities, mechanism and its sensitive phenol sensing based on inhibition of sulfite oxidase mimics. Journal of Hazardous Materials, 2022, 425, 128053.	12.4	21
3	Bimetallic copper-cerium nanoclusters: Assembly-induced aggregation into nanowire network and cysteine-triggered strong red fluorescence turn-on for highly sensitive and selective cysteine sensing. Sensors and Actuators B: Chemical, 2022, 356, 131356.	7.8	4
4	A membraneless starch/O2 biofuel cell based on bacterial surface regulable displayed sequential enzymes of glucoamylase and glucose dehydrogenase. Biosensors and Bioelectronics, 2022, 207, 114197.	10.1	6
5	Vanadium nitride@carbon nanofiber composite: Synthesis, cascade enzyme mimics and its sensitive and selective colorimetric sensing of superoxide anion. Biosensors and Bioelectronics, 2022, 210, 114285.	10.1	19
6	Screening of peptide selectively recognizing prostate-specific antigen and its application in detecting total prostate-specific antigen. Sensors and Actuators B: Chemical, 2022, 367, 132009.	7.8	19
7	Sensitive electrochemical sequential enzyme biosensor for glucose and starch based on glucoamylase- and glucose oxidase-controllably co-displayed yeast recombinant. Analytica Chimica Acta, 2022, 1221, 340173.	5.4	5
8	Hybrid of NiO-Ni12P5/N-doped carbon nanotubes as non-noble electrocatalyst for efficient hydrogen evolution reaction. Colloids and Surfaces A: Physicochemical and Engineering Aspects, 2021, 608, 125613.	4.7	9
9	The <i>in situ</i> growth of Cu ₂ O with a honeycomb structure on a roughed graphite paper for the efficient electroreduction of CO ₂ to C ₂ H ₄ . Catalysis Science and Technology, 2021, 11, 6742-6749.	4.1	8
10	Facile one-pot synthesis of Mn ₃ O ₄ nanorods and their analytical application. New Journal of Chemistry, 2021, 45, 17576-17583.	2.8	2
11	Specific heptapeptide screened from pIII phage display library for sensitive enzyme-linked chemiluminescence immunoassay of vascular endothelial growth factor. Sensors and Actuators B: Chemical, 2021, 333, 129555.	7.8	19
12	Green electroless plating of cuprous oxide nanoparticles onto carbon nanotubes as efficient electrocatalysts for hydrogen evolution reaction. Applied Surface Science, 2021, 548, 149218.	6.1	11
13	A simple electrochemical immunosensor based on worm-like platinum for highly sensitive determination of alpha-fetoprotein. Bioelectrochemistry, 2021, 140, 107804.	4.6	15
14	Copper sulfide nanoclusters with multi-enzyme-like activities and its application in acid phosphatase sensing based on enzymatic cascade reaction. Talanta, 2021, 233, 122594.	5.5	35
15	CuxO nanorods with excellent regenerable NADH peroxidase mimics and its application for selective and sensitive fluorimetric ethanol sensing. Analytica Chimica Acta, 2021, 1186, 339126.	5.4	14
16	Cobalt-doped MoS2 nanocomposite with NADH oxidase mimetic activity and its application in colorimetric biosensing of NADH. Process Biochemistry, 2021, 111, 178-185.	3.7	18
17	Gold nanoplates with superb photothermal efficiency and peroxidase-like activity for rapid and synergistic antibacterial therapy. Chemical Communications, 2021, 57, 1133-1136.	4.1	46
18	Selective colorimetric sensing of sub-nanomolar Hg ²⁺ based on its significantly enhancing peroxidase mimics of silver/copper nanoclusters. Analyst, The, 2021, 146, 4630-4635.	3.5	20

#	Article	IF	CITATIONS
19	Amplified Peroxidaseâ€like Activity of Co ²⁺ Using 8â€Hydroxyquinoline and Its Application for Ultrasensitive Colorimetric Detection of Clioquinol. Chemistry - an Asian Journal, 2021, 16, 3957-3962.	3.3	6
20	Amorphous nickel coating on carbon nanotubes supported Pt nanoparticles as a highly durable and active electrocatalyst for methanol oxidation reaction. Journal of Electroanalytical Chemistry, 2020, 856, 113739.	3.8	20
21	MnO2/multi-walled carbon nanotubes based nanocomposite with enhanced electrocatalytic activity for sensitive amperometric glucose biosensing. Journal of Electroanalytical Chemistry, 2020, 878, 114602.	3.8	19
22	Histidine-triggered turning-on of gold/copper nanocluster fluorescence for the sensitive and selective detection of histidine. Chemical Communications, 2020, 56, 11637-11640.	4.1	28
23	Facile Preparation of Homogeneous Copper Nanoclusters Exhibiting Excellent Tetraenzyme Mimetic Activities for Colorimetric Glutathione Sensing and Fluorimetric Ascorbic Acid Sensing. ACS Applied Materials & Interfaces, 2020, 12, 42521-42530.	8.0	119
24	Facile synthesis of magnetic hierarchical flower-like Co3O4 spheres: Mechanism, excellent tetra-enzyme mimics and their colorimetric biosensing applications. Biosensors and Bioelectronics, 2020, 165, 112342.	10.1	111
25	Ocean green tide derived hierarchical porous carbon with bi-enzyme mimic activities and their application for sensitive colorimetric and fluorescent biosensing. Sensors and Actuators B: Chemical, 2020, 312, 127979.	7.8	39
26	Colorimetric Assay of Bacterial Pathogens Based on Co ₃ O ₄ Magnetic Nanozymes Conjugated with Specific Fusion Phage Proteins and Magnetophoretic Chromatography. ACS Applied Materials & Interfaces, 2020, 12, 9090-9097.	8.0	95
27	Boosting the Peroxidaseâ€like Activity of Cobalt Ions by Amino Acidâ€based Biological Species and Its Applications. Chemistry - an Asian Journal, 2020, 15, 1067-1073.	3.3	3
28	Controllable Display of Sequential Enzymes on Yeast Surface with Enhanced Biocatalytic Activity toward Efficient Enzymatic Biofuel Cells. Journal of the American Chemical Society, 2020, 142, 3222-3230.	13.7	58
29	Tumor Microenvironment-Directed Multisensitive Nanorobotics for Synergistic Photothermal Therapy/Chemotherapy. ACS Applied Bio Materials, 2020, 3, 3345-3353.	4.6	4
30	Tackling the Challenges of Enzymatic (Bio)Fuel Cells. Chemical Reviews, 2019, 119, 9509-9558.	47.7	321
31	Rock salt type NiCo2O3 supported on ordered mesoporous carbon as a highly efficient electrocatalyst for oxygen evolution reaction. Applied Catalysis B: Environmental, 2019, 256, 117852.	20.2	96
32	CoOx/MoOy-anchored multi-wrinkled biomass carbon as a promising material for rapidly selective methyl blue removal. Journal of Materials Science, 2019, 54, 11024-11036.	3.7	11
33	Green tide biomass templated synthesis of molybdenum oxide nanorods supported on carbon as efficient nanozyme for sensitive glucose colorimetric assay. Sensors and Actuators B: Chemical, 2019, 296, 126517.	7.8	70
34	Recent advances in the synthesis of spherical and nanoMOF-derived multifunctional porous carbon for nanomedicine applications. Coordination Chemistry Reviews, 2019, 391, 69-89.	18.8	58
35	CoO-supported ordered mesoporous carbon nanocomposite based nanozyme with peroxidase-like activity for colorimetric detection of glucose. Process Biochemistry, 2019, 81, 92-98.	3.7	69
36	Rock salt type NiO assembled on ordered mesoporous carbon as peroxidase mimetic for colorimetric assay of gallic acid. Talanta, 2019, 201, 406-412.	5.5	42

#	Article	IF	CITATIONS
37	V ₄ P _{6.98} /VO(PO ₃) ₂ as an Efficient Nonâ€Noble Metal Catalyst for Electrochemical Hydrogen Evolution in Alkaline Electrolyte. ChemElectroChem, 2019, 6, 1329-1332.	3.4	8
38	Functional cell surface displaying of acetylcholinesterase for spectrophotometric sensing organophosphate pesticide. Sensors and Actuators B: Chemical, 2019, 279, 483-489.	7.8	26
39	Selected landscape phage probe as selective recognition interface for sensitive total prostate-specific antigen immunosensor. Biosensors and Bioelectronics, 2018, 106, 1-6.	10.1	34
40	Sensitive colorimetric immunoassay of <i>Vibrio parahaemolyticus</i> based on specific nonapeptide probe screening from a phage display library conjugated with MnO ₂ nanosheets with peroxidase-like activity. Nanoscale, 2018, 10, 2825-2833.	5.6	60
41	Facile Synthesis of Water-Dispersed Photoluminescent Gold(I)-Alkanethiolate Nanoparticles via Aggregation-Induced Emission and Their Application in Cell Imaging. ACS Applied Nano Materials, 2018, 1, 6641-6648.	5.0	7
42	Recent advances in gold nanostructures based biosensing and bioimaging. Coordination Chemistry Reviews, 2018, 370, 1-21.	18.8	67
43	Novel Cell–Inorganic Hybrid Catalytic Interfaces with Enhanced Enzymatic Activity and Stability for Sensitive Biosensing of Paraoxon. ACS Applied Materials & Interfaces, 2017, 9, 6894-6901.	8.0	38
44	Phage capsid protein-directed MnO ₂ nanosheets with peroxidase-like activity for spectrometric biosensing and evaluation of antioxidant behaviour. Chemical Communications, 2017, 53, 5216-5219.	4.1	94
45	Novel biotemplated MnO2 1D nanozyme with controllable peroxidase-like activity and unique catalytic mechanism and its application for glucose sensing. Sensors and Actuators B: Chemical, 2017, 252, 919-926.	7.8	107
46	An integrated device of enzymatic biofuel cells and supercapacitor for both efficient electric energy conversion and storage. Electrochimica Acta, 2017, 245, 303-308.	5.2	42
47	Gold nanostructures with near-infrared plasmonic resonance: Synthesis and surface functionalization. Coordination Chemistry Reviews, 2017, 336, 28-42.	18.8	71
48	An efficient strategy to synthesize a multifunctional ferroferric oxide core@dye/SiO ₂ @Au shell nanocomposite and its targeted tumor theranostics. Journal of Materials Chemistry B, 2017, 5, 8209-8218.	5.8	21
49	Sensitive detection of maltose and glucose based on dual enzyme-displayed bacteria electrochemical biosensor. Biosensors and Bioelectronics, 2017, 87, 25-30.	10.1	58
50	Gold nanoprobe functionalized with specific fusion protein selection from phage display and its application in rapid, selective and sensitive colorimetric biosensing of Staphylococcus aureus. Biosensors and Bioelectronics, 2016, 82, 195-203.	10.1	93
51	Genetically Engineered Phage-Templated MnO ₂ Nanowires: Synthesis and Their Application in Electrochemical Glucose Biosensor Operated at Neutral pH Condition. ACS Applied Materials & Interfaces, 2016, 8, 13768-13776.	8.0	106
52	A sensitive acetylcholinesterase biosensor based on gold nanorods modified electrode for detection of organophosphate pesticide. Talanta, 2016, 156-157, 34-41.	5.5	100
53	A Label-Free Electrochemical Impedance Cytosensor Based on Specific Peptide-Fused Phage Selected from Landscape Phage Library. Scientific Reports, 2016, 6, 22199.	3.3	70
54	Microbial surface displaying formate dehydrogenase and its application in optical detection of formate. Enzyme and Microbial Technology, 2016, 91, 59-65.	3.2	16

#	Article	IF	CITATIONS
55	Rational design of xylose dehydrogenase for improved thermostability and its application in development of efficient enzymatic biofuel cell. Enzyme and Microbial Technology, 2016, 84, 78-85.	3.2	26
56	A V2O3-ordered mesoporous carbon composite with novel peroxidase-like activity towards the glucose colorimetric assay. Nanoscale, 2015, 7, 11678-11685.	5.6	100
57	Amperometric l-glutamate biosensor based on bacterial cell-surface displayed glutamate dehydrogenase. Analytica Chimica Acta, 2015, 884, 83-89.	5.4	54
58	Au@Ag Heterogeneous Nanorods as Nanozyme Interfaces with Peroxidase-Like Activity and Their Application for One-Pot Analysis of Glucose at Nearly Neutral pH. ACS Applied Materials & Interfaces, 2015, 7, 14463-14470.	8.0	237
59	Microbial surface displayed enzymes based biofuel cell utilizing degradation products of lignocellulosic biomass for direct electrical energy. Bioresource Technology, 2015, 192, 821-825.	9.6	18
60	Leaf-templated synthesis of 3D hierarchical porous cobalt oxide nanostructure as direct electrochemical biosensing interface with enhanced electrocatalysis. Biosensors and Bioelectronics, 2015, 63, 145-152.	10.1	154
61	Co-immobilization of glucoamylase and glucose oxidase for electrochemical sequential enzyme electrode for starch biosensor and biofuel cell. Biosensors and Bioelectronics, 2014, 51, 158-163.	10.1	57
62	Specific Probe Selection from Landscape Phage Display Library and Its Application in Enzyme-Linked Immunosorbent Assay of Free Prostate-Specific Antigen. Analytical Chemistry, 2014, 86, 2767-2774.	6.5	94
63	Enhanced Performance of a Glucose/O ₂ Biofuel Cell Assembled with Laccase-Covalently Immobilized Three-Dimensional Macroporous Gold Film-Based Biocathode and Bacterial Surface Displayed Glucose Dehydrogenase-Based Bioanode. Analytical Chemistry, 2014, 86, 6057-6063.	6.5	46
64	Specific ligands for classical swine fever virus screened from landscape phage display library. Antiviral Research, 2014, 109, 68-71.	4.1	27
65	Porous gold cluster film prepared from Au@BSA microspheres for electrochemical nonenzymatic glucose sensor. Electrochimica Acta, 2014, 138, 109-114.	5.2	82
66	Peptide Microarray with Ligands at High Density Based on Symmetrical Carrier Landscape Phage for Detection of Cellulase. Analytical Chemistry, 2014, 86, 5844-5850.	6.5	30
67	Bio-mimetic Nanostructure Self-assembled from Au@Ag Heterogeneous Nanorods and Phage Fusion Proteins for Targeted Tumor Optical Detection and Photothermal Therapy. Scientific Reports, 2014, 4, 6808.	3.3	60
68	Microbial surface display of glucose dehydrogenase for amperometric glucose biosensor. Biosensors and Bioelectronics, 2013, 45, 19-24.	10.1	71
69	Simultaneously improving stability and specificity of cell surface displayed glucose dehydrogenase mutants to construct whole-cell biocatalyst for glucose biosensor application. Bioresource Technology, 2013, 147, 492-498.	9.6	41
70	Direct energy conversion from xylose using xylose dehydrogenase surface displayed bacteria based enzymatic biofuel cell. Biosensors and Bioelectronics, 2013, 44, 160-163.	10.1	41
71	Yeast Surface Displaying Clucose Oxidase as Whole-Cell Biocatalyst: Construction, Characterization, and Its Electrochemical Glucose Sensing Application. Analytical Chemistry, 2013, 85, 6107-6112.	6.5	68
72	Construction of Xylose Dehydrogenase Displayed on the Surface of Bacteria Using Ice Nucleation Protein for Sensitive <scp>d</scp> -Xylose Detection. Analytical Chemistry, 2012, 84, 275-282.	6.5	43

#	Article	IF	CITATIONS
73	Simultaneous voltammetric detection of dopamine and uric acid at their physiological level in the presence of ascorbic acid using poly(acrylic acid)-multiwalled carbon-nanotube composite-covered glassy-carbon electrode. Biosensors and Bioelectronics, 2007, 23, 74-80.	10.1	199
74	Effect of solution pH and ionic strength on the stability of poly(acrylic acid)-encapsulated multiwalled carbon nanotubes aqueous dispersion and its application for NADH sensor. Biosensors and Bioelectronics, 2006, 22, 694-699.	10.1	67
75	Multilayer assembly of calf thymus DNA and poly(4-vinylpyridine) derivative bearing [Os(bpy)2Cl]2+: redox behavior within DNA film. Bioelectrochemistry, 2005, 67, 1-6.	4.6	15
76	Amperometric biosensor based on tyrosinase-conjugated polysacchride hybrid film: Selective determination of nanomolar neurotransmitters metabolite of 3,4-dihydroxyphenylacetic acid (DOPAC) in biological fluid. Biosensors and Bioelectronics, 2005, 21, 809-816.	10.1	98
77	Direct Electrochemistry of Myoglobin in Titanate Nanotubes Film. Analytical Chemistry, 2005, 77, 8068-8074.	6.5	168